Paper III

Mechanism for acoustic leakage in surface-acoustic wave resonators on rotated Y-cut lithium tantalate substrate

J. Koskela, J. V. Knuuttila, P. T. Tikka, C. S. Hartmann, V. P. Plessky, and M. M. Salomaa

Mechanism for acoustic leakage in surface-acoustic wave resonators on rotated Y-cut lithium tantalate substrate

J. Koskela, J. V. Knuuttila, P. T. Tikka, C. S. Hartmann,[a] V. P. Plessky,[b] and M. M. Salomaa

Materials Physics Laboratory, Helsinki University of Technology, P.O. Box 2200, FIN-02015 HUT, Finland

We discuss an acoustic loss mechanism in surface-acoustic wave resonators on 36° YX-cut lithium tantalate substrate. Recent acoustic field scans performed with an optical Michelson interferometer reveal a spatially asymmetric acoustic field atop the busbars of a resonator, giving rise to acoustic beams which escape the resonator area and lead to undesired losses. Here, we link the phenomenon with the inherent crystalline anisotropy of the substrate: the shape of the slowness curves and the asymmetry of the polarization for leaky surface-acoustic waves, propagating at an angle with respect to the crystal X-axis. © *1999 American Institute of Physics.* [S0003-6951(99)01843-4]

Surface-acoustic wave (SAW) filters operating on radio frequencies are widely employed in modern telecommunication systems. Electrical measurements of leaky surface-acoustic wave (LSAW) resonators on rotated Y-cut lithium tantalate (LiTaO$_3$) substrate[1] often feature losses not predicted by the common analysis methods, based on the assumption of an infinite aperture or the paraxial approximation. To directly study the acoustic activity in LSAW devices, we utilize a scanning optical Michelson interferometer[2] which detects the shear vertical component of the mechanical displacement.

Scanning several LSAW resonators fabricated on 36° YX-LiTaO$_3$ by different manufacturers we have found an acoustic leakage mechanism.[3] Figure 1 shows probed images over the acoustic field on a series resonator in an impedance element duplexer at various frequencies. The effect becomes evident close to the resonance frequency. The observed acoustic amplitude is slightly shifted to the right w.r.t the positive crystal X-axis, i.e., parallel to the resonator, and strong amplitudes are observed atop the busbar. Acoustic energy is emitted from the resonator area as beams propagating at an angle of about 4°. For higher frequencies the width of the transversal amplitude profile increases and waves are radiated also from the other busbar. The relative strength of the radiation and the spreading of the emitted beams vary with the frequency.

Our measurements have confirmed that reversing the polarity of the drive voltage does not change the direction of the shift of the acoustic field. The particular device probed in Fig. 1 possesses a thinned 1:3 electrode structure, but the effect and the asymmetry have been observed also in conventional 1:1 structures. Since the phenomenon arises independently of the transversal symmetry of the device, the asymmetry must originate from the substrate crystal itself.

The theoretically computed[4] surface velocities of LSAWs, Rayleigh-type SAWs, and surface-skimming bulk-acoustic waves on rotated Y-cut LiTaO$_3$ are symmetric about the X-axis.[5] However, the polarizations of the LSAWs are asymmetric.[6] The normalized polarization on a metallized surface is illustrated in Fig. 2 as a function of the propagation angle.

The dominating shear horizontal component (U_2) is almost symmetric about the X-axis but, compared to the electric potential, features a linearly deviating phase as a function of the propagation angle. Such behavior has been shown to lead to a constant shift of the acoustic transduction amplitude with respect to the electric source.[7] However, the shift appears to be too weak (about 0.12 wavelengths) to explain the observed amplitude pattern.

The waves also contain weak longitudinal (U_1) and shear vertical (U_3) components. According to Fig. 2, these are asymmetric functions of the propagation angle, both in magnitude and in phase. Consequently, the waveguide
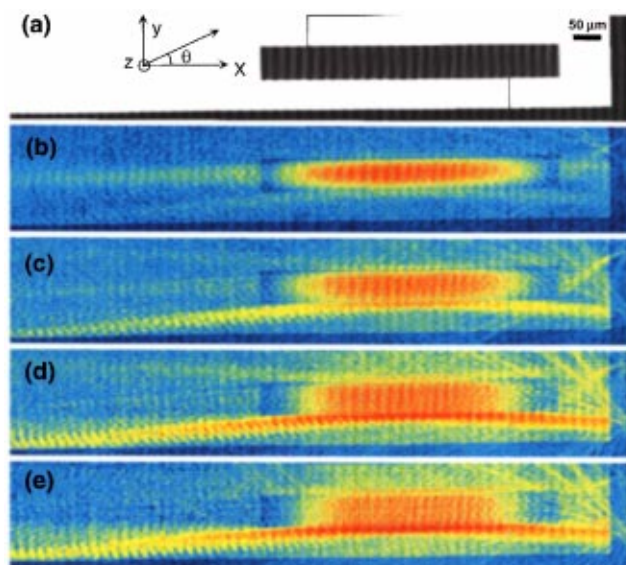

FIG. 1. Area scans of a series resonator in a low-loss IEF filter: (a) light-reflection data at each scanning point, and the acoustic field for the frequencies, (b) 925 MHz (resonance), (c) 927 MHz, (d) 929 MHz, and (e) 933 MHz. The amplitudes are not in scale for areas with different light reflection coefficients.

[a]RF SAW Components, Inc., 6110 East Mockingbird Lane, Suite 102-762, Dallas, TX 75214-2600.
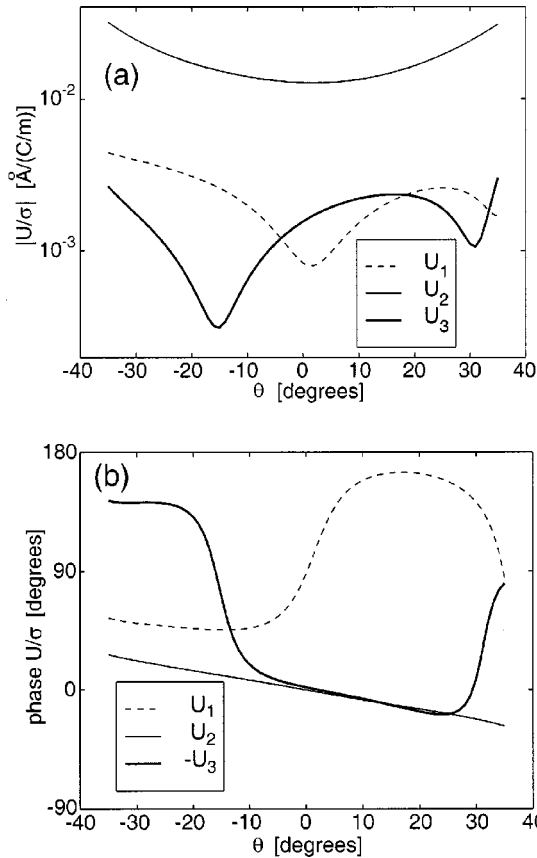[b]Thomson Microsonics, SAW Design Bureau, Fahys 9, CH-2000 Neuchâtel, Switzerland.

FIG. 2. Computed polarization for LSAWs propagating on a metallized crystal surface at an angle θ with respect to the crystal X-axis: (a) the relative magnitude and (b) the relative phase of components of mechanical displacement, normalized to the charge density (σ).
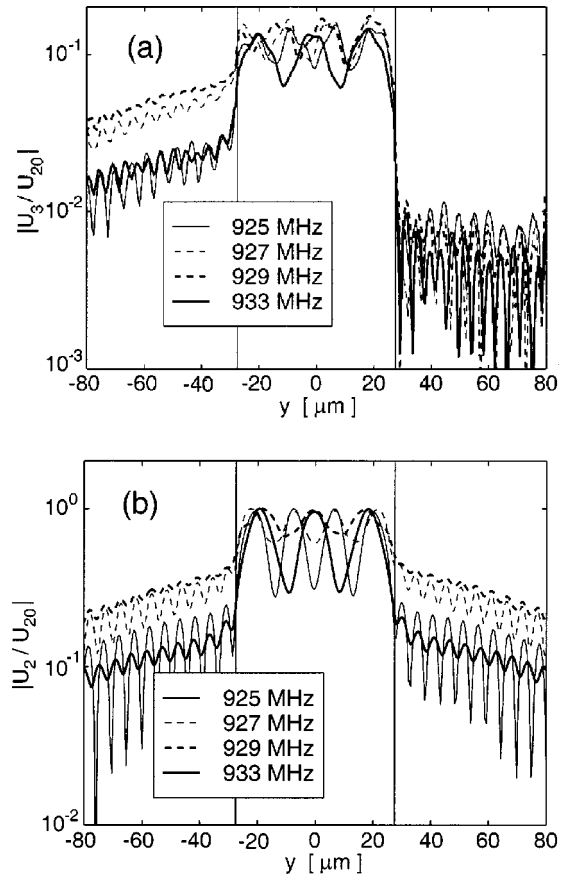
FIG. 3. Computed transversal profiles of mechanical displacements arising from a rectangular voltage wave: (a) shear vertical and (b) shear horizontal component.

modes excited in a symmetric structure are likely to possess a strong asymmetry in the shear vertical component of the displacement.

To obtain rough quantitative understanding of the effect of the crystal anisotropy on LSAW resonators with a finite aperture, Fourier transformation techniques and the Green's function method[8] were utilized to compute the mechanical displacement field arising from the voltage wave

$$\Phi(x,y) = \Theta\left(1 - \frac{2|y|}{W}\right)e^{-i\pi x/p}. \quad (1)$$

Here, x and y are the main and transverse directions along the surface, $\Theta(y)$ denotes the step function, $W = 55 \, \mu$m is the acoustic aperture, and the pitch $p = 2.163 \, \mu$m is the mechanical periodicity. The dimensions were chosen to agree with those of the resonator shown in Fig. 1.

The voltage wave [Eq. (1)] approximates the dominating forward-propagating Fourier component of the voltage field inside a long resonator surrounded by wide busbars and operating at the stopband frequencies. However, several phenomena, such as the wave guidance due to mass loading and the interaction between the counterpropagating wave components, are not taken into account.

The transversal amplitude profiles obtained for the scanned frequencies are displayed in Fig. 3. Despite the very approximate nature of the model, in agreement with the scans the shear vertical displacement outside the source region is considerably larger along $-y$ than along $+y$. The

profile of the dominating shear horizontal component is almost symmetric. This suggests that—despite the asymmetry observed with the laser probe—acoustic leakage actually occurs on both sides of the resonator. The relative amplitude levels and the degree of the asymmetry outside the structure depend strongly on frequency. On the other hand, in the source region the estimated profiles weakly agree with the experiments. A more realistic model is clearly required.

The images shown in Fig. 1 reveal that the acoustic field in the active region of the resonator remains practically confined in the longitudinal direction. However, the field on the busbars is free to escape the device. The propagation characteristics observed may be understood based on the slowness curve for the LSAWs on a metallized surface, depicted in Fig. 4(a). The curve features both convex and concave regions. Consequently, the direction of the energy flow varies significantly with the propagation angle [see Fig. 4(b)].

Since the scanning frequencies f are within the stopband of the resonator, the dominating Fourier components of the acoustic field propagate with slownesses $s_x = \pm 1/(2pf)$ along X. As indicated in Fig. 4(b), the metallized crystal surface supports two LSAW modes with energy propagating at about an angle of $\pm(4°-7°)$ and $\pm(6°-12°)$ about X. This well suits with the average direction and the spreading of the acoustic beams observed by the laser probe. Consequently, the beams are identified as LSAWs escaping from the resonator.

Figure 4 implies that, in addition to the LSAWs, Rayleigh-type surface-acoustic waves and fast shear bulk-

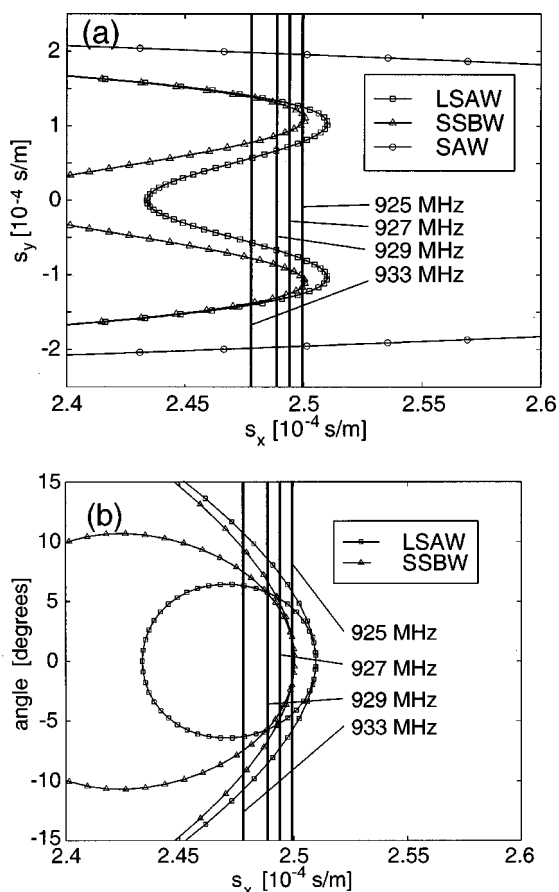Appl. Phys. Lett., Vol. 75, No. 17, 25 October 1999

Koskela *et al.* 2685

FIG. 4. (a) Slowness curves and (b) the direction of energy flow for LSAWs and Rayleigh-type SAWs on a metallized surface, and for fast shear bulk-acoustic waves with the energy propagating along the surface. Vertical lines indicate the slownesses dominating at the scanning frequencies.

acoustic waves propagating with an energy flow along the surface are also radiated at all the scanned frequencies. These are expected to cause the weak acoustic background observed in the probe images. Indeed, scans of larger surface areas show very slowly attenuating acoustic beams propagating at about an angle of 40° with respect to the resonator.

Based on these properties, they are identified as Rayleigh waves.

In conclusion, we analyze a leakage mechanism in LSAW resonators on rotated Y-cut LiTaO₃ substrates. Laser-interferometric scans reveal that part of the acoustic field excited in the resonator escapes the device through the bus-bars, causing undesired acoustic losses at the operation frequencies of the resonator. We explain the effect with the metallized crystal surface supporting LSAWs and fast shear bulk waves, capable of transferring energy away from the busbars. In accordance with the probe images, theoretical estimates using a simplified model predict that the shear vertical component of the acoustic field radiated is spatially asymmetric and that the effect depends strongly on frequency. Further investigations of the mechanism and its occurrence in other substrates, and a more detailed model are required to find design principles to minimize the leakage.

[1] H. H. Ou, N. Inose, and N. Sakamoto, *Proceedings of the 1998 IEEE Ultrasonics Symposium* (IEEE, New York, 1998), p. 97.

[2] J. V. Knuuttila, P. T. Tikka, T. Thorvaldsson, V. P. Plessky, and M. M. Salomaa, *Proceedings of the 1997 IEEE Ultrasonics Symposium* (IEEE, New York, 1997), p. 161.

[3] J. V. Knuuttila, P. T. Tikka, C. S. Hartmann, V. P. Plessky, and M. M. Salomaa, Electron. Lett. **35**, 1115 (1999).

[4] In all calculations, the materials parameters for LiTaO₃ crystal are taken from Ref. 5.

[5] G. Kovacs, M. Anhorn, H. E. Engan, G. Visintini, and C. C. W. Ruppel, *Proceedings of the 1990 IEEE Ultrasonics Symposium* (IEEE, New York, 1990), p. 435.

[6] This surprising occurrence of asymmetric wave polarization related with unmistakably symmetric LSAW wave velocity is associated with the very small leakage of the LSAW into shear bulk-acoustic waves. The Rayleigh waves on this same cut exhibit symmetry about the X-axis for both velocity and polarization.

[7] C. S. Hartmann, B. P. Abbott, S. Jen, and D. P. Chen, *Proceedings of the 1994 IEEE Ultrasonics Symposium* (IEEE, New York, 1994), p. 71.

[8] R. C. Peach, *Proceedings of the 1995 IEEE Ultrasonics Symposium* (IEEE, New York, 1995), p. 221.